https://doi.org/10.5194/bg-2019-389
Preprint. Discussion started: 4 November 2019

Biogeosciences Discussions
Open Access
EGU

The influences of historic lake trophy and mixing regime changes on long-term phosphorus fractions retention in sediments of deep, eutrophic lakes: a case study from Lake Burgäschi, Switzerland

Luyao Tu[1], Paul Zander[1], Sönke Szidat[2], Ronald Lloren[3,4], Martin Grosjean[1]

1 Oeschger Centre for Climate Change Research and Institute of Geography, University of Bern, Switzerland
2 Oeschger Centre for Climate Change Research and Department of Chemistry and Biochemistry, University of Bern, Switzerland
3 Department of Earth Science, ETH Zürich, Switzerland
4 Eawag, Swiss Federal Institute of Aquatic Science and Technology, Switzerland

Correspondence to: Luyao Tu (luyao.tu@giub.unibe.ch)

Abstract. Hypolimnetic anoxia in eutrophic lakes can delay lake recovery to lower trophic states via the release of sediment phosphorus (P) to surface waters on short time scales. However, the effects of hypolimnetic redox conditions and eutrophication on long-term sediment P-fraction retention are not clear yet. In this study, we investigated the sediment profiles since the early 1900s from Lake Burgäschi, a deep, eutrophic lake on the Swiss Plateau. The changes of sediment P-fraction retention were assessed with respect to lake trophic evolution (sedimentary green-pigments proxy), hypolimnetic oxygenation regime (Fe/Mn ratio proxy), sediment geochemical characteristics, and lake restoration history. Results showed that long-term retention of total P and labile P-fractions in sediments was predominantly affected by autochthonous Fe and Mn preserved in anoxic sediments, which were controlled by past hypolimnetic redox conditions. By contrast, refractory HCl-P (Ca-P) fraction retention largely resulted from authigenic $CaCO_3$-P precipitation and increased with higher eutrophic levels. The retention of total P and labile P fractions was considerably reduced in surface sediments from 1977-2017, when Lake Burgäschi had the highest eutrophic levels and a persistent anoxic hypolimnion. We attributed the phenomenon to reduced sediment P-binding capacity (Mn and Fe oxyhydroxides) under the eutrophication-induced anoxic hypolimnion and decreased water-P concentrations due to hypolimnetic withdrawal. Our study implies that in seasonally stratified deep lakes like Lake Burgäschi, hypolimnetic withdrawal of P-enriched water can effectively reduce P retention in sediments and potentials of sediment-P release (seen from low P availability after 1977). However, the restoration has not improved lake trophic state, similarly to the findings from lake limnological survey.

Keywords: Phosphorus fractions, eutrophication, hypolimnetic anoxia, hypolimnetic withdrawal, deep lakes

https://doi.org/10.5194/bg-2019-389
Preprint. Discussion started: 4 November 2019

1 Introduction

Phosphorus (P) eutrophication in freshwater lakes is a global problem and has been a matter of concern to the public for several decades. In lakes where the external P loading has been reduced, internal P loading (sediment-P release to surface waters) is widely recognized as the key factor affecting lake trophic status and delaying lake recovery from eutrophication (Burley et al., 2001; Trolle et al., 2010). Considerable work has been done on sediment-P speciation to evaluate sediment-P release potentials and implications for lake restoration management (Gonsiorczyk et al., 1998; Ribeiro et al., 2008).

The paradigm that oxygen controls the sediment-P release via reductive dissolution of Fe-P fraction in surface sediments has been accepted as the classical model for a long time (Einsele, 1936, 1938; Moosmann et al., 2006), which was supported by numerous short-term (days or seasonal) laboratory or in-situ studies (Chen et al., 2018). Based on this paradigm, it was assumed that an oxic sediment–water interface might limit the release of Fe-P from sediments and, therefore, improve P retention in lake sediments. However, the restoration measures with artificial hypolimnetic oxygenation/aeration applied in eutrophic lakes proved to have only short-lasting effects but no direct effects on internal P loading and redox-dependent sediment-P retention on longer terms (Gächter, 1987; Gächter and Wehrli, 1998; Moosmann et al., 2006; Hupfer and Lewandowski, 2008). Gächter and Müller (2003) and Moosmann et al. (2006) further argued that, on multi-decadal or longer time scales, P retention in lake sediments might eventually primarily depend on the P-binding capacity of anoxic sediments and sediment composition (e.g. Fe, Mn, Al, and Ca contents). Nevertheless, until now, there is a lack of evidence from well-dated sediment cores, and there is still a need to know which processes may have a dominant influence on sediment P-fraction retention on longer time scales (e.g., decades or more). This information is crucial for predicting and, ultimately, managing sediment-P release, especially in deep lakes, because hypolimnetic anoxia in deep lakes can lead to large loads of sediment-P release. Furthermore, eutrophication has been demonstrated to affect sediment-P release via controlling hypolimnetic anoxia and lake mixing regime in seasonally stratified deep lakes (Tu et al., 2019). It is not yet fully understood whether and how lake trophic levels and hypolimnetic anoxia can influence the long-term behavior of sedimentary P-fraction retention in deep lakes.

The restoration technique of hypolimnetic water withdrawal has been frequently applied in seasonally stratified lakes in Europe (Kucklentz and Hamm, 1988; Nürnberg, 2007), whereby P-enriched water from the hypolimnion is discharged directly into the lake outflow. This restoration technique has been shown to efficiently reduce P concentrations in lake waters (Nürnberg, 2007). However, the long-term influence of this restoration on sedimentary P-fraction retention is unclear.

The objectives of this study were to (1) explore the main factors controlling long-term changes of P-fraction retention in sediments of deep lakes, (2) investigate how sediment P-fraction retention responds to changes in lake eutrophication and hypolimnetic anoxia of the past prior to anthropogenic eutrophication, and (3) examine the effects of lake hypolimnetic withdrawal restoration on sedimentary P-fraction retention. To achieve these objectives, we investigated short sediment cores from Lake Burgäschi, a deep and eutrophic lake on the Swiss Plateau. Sedimentary green-pigments s (chlorophylls and diagenetic products) inferred from hyperspectral imaging (HSI) scanning and XRF-inferred Fe/Mn ratios primarily reflect lake trophic state evolution (aquatic primary productivity) and hypolimnetic oxygenation, respectively. A sequential P-extraction with five P fractions was

https://doi.org/10.5194/bg-2019-389
Preprint. Discussion started: 4 November 2019

performed to uncover P fractionation in sediment profiles. We combined all data to identify the dominant factors responsible for temporal changes in P-fraction retention. Changes in P-fraction records for the periods before and during the restoration were also investigated.

Lake Burgäschi is an excellent study site because there were substantial changes in lake trophic levels and possibly lake-mixing regimes since the last century (Guthruf et al., 1999; van Raden, 2012), and exceptionally long historical and limnological survey data are available for most of the last 50 years. Hypolimnetic withdrawal restoration has operated in the lake since 1977.

2 Study site

Lake Burgäschi (47°10′8.5″N, 7°40′5.9″E) is a small lake located on the Swiss Plateau (Fig. 1a). It has a very restricted catchment (3.2 km^2). The catchment area geologically belongs to the Molasse Basin, and mostly consists of carbonate-rich sandstones and mudstones (Schmid et al., 2004). The kettle hole lake was formed after the retreat of the Rhone glacier (ca. 19 k yr. BP; Rey et al., 2017) and, today, has a maximum water depth of ~31 m, which is quite deep in contrast to the small surface area of 0.21 km^2 (Guthruf et al., 1999). The mean retention time of the lake water is ~1.4 year (Nürnberg, 1987). The lake has several small inflows in the southwest (Rey et al., 2017) and one outflow in the north (Fig. 1c).

Since the 19th century, the lake's water level was lowered several times to create agricultural lands, with the most lowering (up to 2 m) during 1943-1945 (Guthruf et al., 1999). Agricultural area currently covers ~55% of the lake catchment, followed by ~29% area of forests. The lake region experiences a warm humid continental climate (Dfb; Köppen-Geiger classification). The mean annual temperature is 9 °C and the warmest month is July (mean temperature 19 °C).

Lake Burgäschi has been highly productive (eutrophic to highly eutrophic state) since the 1970s with high algal-biomass production and anoxic conditions in the hypolimnion (Guthruf et al., 1999, 2013). The eutrophication in Lake Burgäschi has been linked to increased agricultural P inputs via drainage into the lake in the second half of the 20th century (Guthruf et al., 1999). To mitigate the eutrophication, hypolimnetic withdrawal restoration has been applied in Lake Burgäschi since 1977, and the lake water has been monitored twice a year for more than 30 years for various parameters, such as pH, oxygen content, phosphorus concentrations, phytoplankton biomass etc. Despite a sharp decline in hypolimnetic phosphorus concentrations due to the restoration, a high production of algae biomass continues today. Additionally, hypolimnetic oxygenation conditions and the lake trophic state have been stabilized but not fundamentally improved (Markus, 1995; Guthruf et al., 2013).

3 Materials and methods

3.1 Core collection and sampling

In September 2017, two 75-cm-long sediment cores (Burg17-B and Burg17-C) were retrieved from the deepest point of Lake Burgäschi (water depth ~31 m) (47°10'8.6"N, 07°40'5.3"E; coring site in Fig. 1c) using a UWITEC

https://doi.org/10.5194/bg-2019-389
Preprint. Discussion started: 4 November 2019

gravity corer. After the collection, the cores were stored in a dark cold room (~4 °C). After opening and splitting lengthwise, core-half A of Burg17-B was continuously subsampled at 2-cm resolution from 0 to 60 cm for ^{210}Pb and ^{137}Cs dating (section 3.2). The oxidized surface of core-half B (Burg17-B) was visually described (Schnurrenberger et al., 2003) before non-destructive XRF core and HSI scanning (Section 3.3). After the opening, one-half of core Burg17-C was transferred immediately into a glove box with an anoxic atmosphere where it was continuously subsampled at 2-cm resolution from 0 to 72 cm. The fresh sediments from each sample slice were homogenized and used for sequential P extraction. Afterwards, the remaining sediment was freeze-dried and homogenized for bulk element analyses (Section 3.4).

3.2 Chronology

The chronology of the core Burg17-B is based on ^{210}Pb and ^{137}Cs activity profiles. The freeze-dried and homogeneous samples were stored dry and dark until analysis. The ^{210}Pb, ^{137}Cs and ^{226}Ra radiometric activities were measured by gamma spectrometry conducted at the Department of Chemistry and Biochemistry at University of Bern. 1.3-5.1 g of the freeze-dried samples were encapsulated into polystyrene petri dishes (68 mm O.D., 11 mm height; Semadeni, Ostermundigen, Switzerland) together with a polystyrene disk to fill in the headspace above the material and the petri dishes were vacuum-sealed into a gas-tight aluminum foil. ^{210}Pb (46.5 keV), ^{241}Am (59.5 keV), ^{226}Ra progenies ^{214}Pb and ^{214}Bi (295.2, 351.9 and 609.3 keV), as well as ^{137}Cs (661.7 keV) were measured using a Broad Energy Germanium (BEGe) detector (Canberra GmbH, Rüsselsheim, Germany). This system is composed of a high-purity germanium crystal of 50 cm^2 area and 30 mm thickness with a 0.6 mm thick carbon epoxy window, which shows high absolute full-energy peak efficiencies for close on-top geometries of >20% and ~5% for ^{210}Pb and ^{137}Cs, respectively. Low integrated background count rates of 0.20 s^{-1} (energy range of 30-1800 keV) were achieved by application of low-background materials, installation in third underground floor (~10 m of water-equivalent overburden), passive shielding (outside to inside: 10 cm low-background lead, 3 mm ancient lead with negligible ^{210}Pb content, 2 mm cadmium), flushing of the shield interior with nitrogen gas and an active anti-cosmic shield (plastic scintillator panels of totally 1 m^2 area mounted directly above the passive shielding). Supported ^{210}Pb in each sample was assumed to be in equilibrium with the in-situ ^{226}Ra (equilibration time 4 weeks). Unsupported ^{210}Pb activity was calculated by subtracting ^{226}Ra activity from total ^{210}Pb activity level-by-level. The correction for the total unsupported ^{210}Pb missing inventory followed Tylmann et al. (2016).

The ^{210}Pb chronology of Core Burg17-B was determined using the Constant Rate of Supply (CRS) model (Appleby, 2002), which accounts for variation in sediment accumulation rates. We tested two CRS models: CRS-1 model was unconstrained (i.e. without reference points from the ^{137}Cs activity). The CRS-2 model was constrained with the chronologic marker of peak fallout from nuclear weapons testing in 1963 (^{137}Cs and ^{241}Am). Both models were then tested and validated with independent time-markers at the onset of nuclear weapons testing in 1953/54 and the Chernobyl accident in 1986/87 (onset of ^{137}Cs and peak of ^{137}Cs and ^{241}Am, respectively).

The two sediment cores (Burg 17-B and Burg 17-C) are visually very similar but show a length-offset due to coring compaction of approximately 2-6 cm (Fig. S1). The age-depth stratigraphy of Burg17-C core was inferred from the dated core Burg17-B by visual stratigraphic correlation from high-resolution core pictures.

https://doi.org/10.5194/bg-2019-389
Preprint. Discussion started: 4 November 2019

149 **3.3 Non-destructive geochemical methods**

150 Non-destructive X-ray fluorescence (XRF) core scanning was done using an Avaatech XRF Core Scanner (Richter
151 et al., 2006) for semi-quantitative element composition measurements at 0.5 mm resolution to capture relative
152 elemental concentrations of the laminae. Core surface was smoothed and covered with a 4-µm-thick Ultralene foil
153 prior to the analysis. Elements were measured using a Rhodium anode and a 25 µm Be window. The lighter
154 elements were measured at 15 seconds count time at 10 kV with 1500 A, no filter; while the heavier elements were
155 exposed at 40 seconds at 30 kV with 2000 A, Pd-thin filter. Element intensities (semi-quantitative concentrations)
156 of the selected elements (Mg, Si, Al, K, Ti, Rb, P, Fe, Mn, Ca) are expressed as count rates (counts per second,
157 cps).

158 Following the methodology in Butz et al. (2015), hyperspectral imaging (HSI) scanning was performed using a
159 Specim Ltd. Single Core Scanner equipped with a visual to near infrared range (VNIR, 400–1000 nm)
160 hyperspectral linescan camera (Specim PFD-CL-65-V10E). Parameters were set for a spatial resolution of ~70
161 µm/pixel and a spectral sampling of 1.57 nm (binning of 2). Spectral endmembers were determined using the
162 "Spectral Hourglass Wizard" of the ENVI 5.5 software package (Exelisvis ENVI, Boulder, Colorado). The relative
163 absorption band depth (RABD) index calculation was performed following the method in Schneider et al. (2018).
164 However, based on the spectral end members (Fig. S2), we used the absorption feature between the wavelengths
165 R590 and R765 (590-765 nm), i.e. $RABD_{590\text{-}765}$. Butz et al. (2017) and Schneider et al. (2018) revealed that this
166 index is well calibrated to absolute green-pigments concentrations (chlorophyll *a* + pheophytin a) in sediments.
167 Therefore, in our study, the relative concentrations of green-pigments inferred from $RABD_{590\text{-}765}$ index values
168 provide a semi-quantitative reconstruction of lake primary productivity (total algal abundance) at sub-annual
169 resolution, and are suggested to reflect the trophic state evolution of Lake Burgäschi.

170 **3.4 Phosphorus fractionation scheme and bulk elements analyses**

171 The P-fractionation extraction protocol principally follows the four-step extraction protocol in Tu et al., (2019). In
172 addition, we added the last extraction step from Lukkari et al. (2007) to determine refractory organic P (F5). This
173 P fraction (F5) is practically biologically unavailable and subject to permanent P burial. The first four fractions
174 are NaCl-TP (F1: loosely bound P), NaBD-TP (F2: redox-sensitive Fe- and Mn-bound P), NaOH-TP (F3: Al- and
175 Fe-bound P), and HCl-TP (F4: Ca-bound P) (Tu et al., 2019), whereby NaCl-TP, NaBD-TP and NaOH-TP
176 fractions together as considered relatively labile P fractions because they may release P back to the water column
177 under anoxic or high pH environments (Rydin, 2000). The HCl-TP and refractory organic P (Ref.-P_o) fractions are
178 classified as relatively stable or refractory P fractions. Total P in sediments was obtained from the sum of the five
179 P fractions. The P in extract samples was measured by inductively coupled plasma mass spectroscopy (7700× ICP-
180 MS) (Agilent Technologies, Germany) after the dilution with nitric acid (HNO_3) to reach a final concentration of
181 1% v/v HNO_3.

182 Concentrations of total carbon (TC), total nitrogen (TN), and total sulfur (S) in sediment samples were determined
183 using an Elementar vario El Cube elemental analyzer. Total inorganic carbon (TIC) content was calculated by
184 multiplying loss on ignition at 950 °C (LOI_{950}, following the method proposed by Heiri et al. (2001)) by 0.273, i.e.
185 the ratio of the molecular weight of C and CO_2. Total organic carbon (TOC) content was calculated using the

https://doi.org/10.5194/bg-2019-389
Preprint. Discussion started: 4 November 2019

equation TOC =TC-TIC. Sediment dry bulk density and water content were determined following the method in Håkanson and Jansson (2002).

3.5 Data analyses

Multivariate statistical analyses were performed with R version 3.4.2 (R Development Core Team, 2017). Prior to data analyses, $RABD_{590\text{-}765}$ index values (resolution 70 µm) were aggregated to a spatial resolution of 0.5 mm (the spatial resolution of XRF data). Stratigraphically constrained incremental sum of squares clustering (CONISS; Grimm, 1987) was then performed on semi-quantitative proxies (i.e. $RADB_{590–765}$ index and XRF-element data) with R-package ''rioja'' (Juggins, 2017). The number of significant clusters was determined with a broken-stick test (Bennett, 1996). A principal components analysis (PCA) was performed on the centered and standardized data of semi-quantitative proxies, using the "Vegan" package (Oksanen et al., 2013). Then after, XRF-element and $RABD_{590\text{-}765}$ index data points within the depth range corresponding to samples taken from core Burg17-C were used to calculate mean values for each sample. In order to identify the primary factors influencing the variations in sedimentary P fractions, a redundancy analysis (RDA) was performed on the centered and standardized dataset of P fractions (response variables) and other sediment geochemical parameters (explanatory variables) with the "vegan" package. In the RDA computation, the correlation matrix option was selected and the scaling was conducted on a correlation biplot.

4 Results

4.1 ^{137}Cs and ^{210}Pb chronology

The two distinctive peaks of ^{137}Cs in sediment profiles are detected at 31 cm and 15 cm depths (Fig. 2b), corresponding to the 1963 and 1986 major fallout events, respectively (Appleby, 2002). Furthermore, ^{241}Am activity peaks at the same depths (Fig. 2b), confirming that the 1963 and 1986 ^{137}Cs peaks were due to atmospheric fallouts (Michel et al., 2001). The first traces of ^{137}Cs occur at 37 cm depth, indicating the first widely detectable fallout from atmospheric nuclear testing in 1953/1954 (Pennington et al., 1973).

The ^{210}Pb activity in Core Burg17-B shows a relatively monotonic decrease down to a sediment depth of 17 cm. Further down, larger variations are found (Fig. 2a). The ^{210}Pb and ^{226}Ra activities do not reach the equilibrium; unsupported ^{210}Pb activity in the oldest sample (59 cm) is still above the limit of detection (14.0±6.8 $Bq \cdot kg^{-1}$). The observed cumulative inventory of unsupported ^{210}Pb is 2941 $Bq \cdot m^{-2}$. We corrected this value (missing inventory correction; Tylmann et al., 2016) by applying an exponential equation using the lowermost values of cumulative dry mass and unsupported ^{210}Pb activity between 8 and 60 cm depths. As a result, a correction value of 125.2 $Bq \cdot m^{-2}$ (missing inventory) is added to the final total unsupported ^{210}Pb inventory (3066 $Bq \cdot m^{-2}$).

The CRS-2 model (constrained through 1963) shows a better agreement with the independent ^{137}Cs markers at 1953/54 and 1986/87 than the CRS-1 model (Fig. 2c). Therefore, CRS-2 model results were chosen for determining the age-depth profile and sediment mass accumulation rates (MAR) of Core Burg17-B. The mean age at 59 cm sediment depth dates back to ~1930. The extrapolated mean age at 61 cm depth is ~1926 calculated using the mean sediment accumulation rate between 54-60 cm (2 $yr \cdot cm^{-1}$).

https://doi.org/10.5194/bg-2019-389
Preprint. Discussion started: 4 November 2019

4.2 Sediment lithology, green-pigments ($RABD_{590-765}$ index) and XRF-element records

Four sediment facies (I to IV, Fig. 3a and 4) are identified based on visual classification and the CONISS-analysis results of XRF-element intensities.

In Zone I (75.4-61cm, pre ~1926), the sediments consist of visible thin brown-to-reddish laminae (Mn- and Fe rich). Green-pigments concentrations inferred from $RABD_{590-765}$ index values show a homogenous distribution with the lowest values within the sediment profile (Fig. 2d). Fe/Mn ratios vary within very low values (mostly below 10). The Mn, Fe, P and Fe/Ti values show high levels with large variability. Extremely low Ca amounts are noted in this zone.

In Zone II (61-34cm, ~1926-1960), the sediments show dark gyttja, partly laminated with light Ca-rich layers. Green-pigments concentrations slightly increase yet still show little variability. A sharp increase of green-pigments concentrations occurs at 60 cm, and the first two local peaks near 55 cm (~1938) and 48 cm (1945) are notable. Fe/Mn ratios remain at slightly higher values than in Zone I. The Mn, Fe, P contents and Fe/Ti values all decline to low levels and remain relatively stable. Ca counts increase gradually over the whole Zone II.

In Zone III (34-21.5 cm, ~1960-1977), the sediments are mostly characterized by brown-to-reddish laminations (Mn-Fe rich), with thicker and more distinct laminae contacts than in Zone I. Green-pigments concentrations exhibit much higher values with positive trends, intensified variability, and several maxima (seasonal algal blooms). Fe/Mn ratios first drop in the lower part (34-27 cm) and then continue to increase upward to the top-part of Zone III. Fe, Mn, P, and Fe/Ti values change with general opposite trends to Fe/Mn ratios. Ca contents are elevated during this period relative to Zones I and II.

In Zone IV (21.5-0 cm, ~1977-2017), the sediments exhibit a clear laminated structure with much more pronounced light calcite layers. The laminations are characterized by a regular succession of light calcite layers (Ca-rich) and dark organic-rich layers (Fig. S3). Green-pigments concentrations display the highest levels with large fluctuations, and reaches distinct local maxima at 18 cm (1981), 15 cm (1985), 13 cm (1987), 12 cm (1988), and 8 cm (1997) depths (Fig. 3b). Fe/Mn ratios remain at similarly high values as in Zone II, yet with more variability. The Fe, Mn, and P element counts and Fe/Ti all show constantly very low values. The Ca amounts are the highest in the profile and show considerabley variability.

Two principle components, PC1 and PC2 were shown to be significant using a broken stick model. They explain ~35 % and ~30 % of the total variance in the dataset, respectively (PCA-biplot; Fig. S4). The PC1 has strong positive loadings for the terrigenous elements (K, Ti, Rb etc.) and thus represents mainly erosional processes related to allochthonous inputs. The PC2 has strong positive loadings for redox-sensitive elements (Fe, Mn), P and Fe/Ti, but negative loadings for Ca, Fe/Mn ratios and green-pigments index values. Therefore, PC2 reflects changes in redox conditions of hypolimnetic water and lake primary productivity. The results of additional PCA analyses zone by zone (Fig. S5b) show that Mn, Fe and P were mostly independent of terrigenous elements (in Zones I to III), however in Zone IV, Mn, Fe and P become correlated with the terrigenous elements. The vertical profile of XRF-P matches very well with the changes of total P concentrations in sediments (Fig. S6). It reveals

https://doi.org/10.5194/bg-2019-389
Preprint. Discussion started: 4 November 2019

that XRF-P data can reliably represent qualitative variations of total P concentrations in sediment profiles of Lake Burgäschi.

4.3 Bulk elements and P fractions in sediment profiles

Sediment TIC, TOC, TOC/TN ratio, S and P fractions also show distinctive features along the four stratigraphic zones (Fig. 5). From the upper part of Zone I (65.2-61 cm; ~1926) to Zone IV, TIC shows a similar pattern to the XRF-Ca contents (Fig. 4 and 5) suggesting that TIC is mostly present in the form of $CaCO_3$. Over the whole profile, TOC/TN ratios are within the range of 9-11. TOC and TOC/TN ratios exhibit mostly similar patterns from Zone I to Zone III. By contrast, total sulfur (S) contents display a different pattern, showing very low values in Zone I and II (mean ~0.5%), and a substantial increase in Zone III and IV.

The concentrations of relatively labile P fractions (i.e. NaCl-TP, NaBD-TP and NaOH-TP) and total P have a similar trend over the whole profile (Fig. 5 and 6a). They all display rather large values during the upper part of Zone I and generally reduced values in Zone II. Afterwards, they increase to peaks at ~25 cm depth but sharply decrease to the lowest values in the upper boundary of Zone III and throughout Zone IV. HCl-TP and Res.-P_o fractions vary differently compared with the other fractions. Low contents of HCl-TP fraction are observed in Zone I and II. HCl-TP fraction has a rather similar pattern as labile P fractions in Zone III, but then it remains at high levels in Zone IV. Res.-P_o fraction contents show relatively stable values from Zone I to Zone II, followed by a gradual rise in Zone III and in the upper part of Zone IV.

Regarding the P composition in sediment profiles (Fig. 6), from Zone I to Zone III (65.2-21.5 cm) NaBD-TP fraction is the most important P-form representing ~50% of total P followed by NaOH-TP fraction. However, in Zone IV (depth above ~ 21.5 cm), HCl-TP becomes the main P fraction (39% of total P) over NaBD-TP (30% of total P).

The relationships between response variables and explanatory variables are visible on the redundancy analysis (RDA) biplot (Fig. 7), which, in most cases, correspond well to the results of Spearman rank correlation test (Fig. S7). The relatively labile P fractions (NaCl-TP, NaBD-TP and NaOH-TP) and total P in sediments are strongly positively correlated with redox-sensitive elements (Fe and Mn) and autochthonous Fe (Fe/Ti). However, these P fractions are negatively related to hypolimnetic oxygenation proxy (Fe/Mn ratios) and, to some extent, to lake productivity indicators (green-pigments, XRF-Ca and TIC). HCl-TP and Ref.-P_o fractions are positively correlated with each other. However, only HCl-TP fraction has close positive relationships with lake productivity indicators.

5 Discussion

5.1 Trophic state evolution of Lake Burgäschi

Four main phases of different lake trophic levels (based on $RABD_{590\text{-}765}$ index record) were distinguished since the early 1900s. During the period prior to ~1926 in Zone I, the lowest green-pigments index values reflect low lake primary productivity. In the early 1900s, agricultural impacts around the catchment area of Lake Burgäschi were

https://doi.org/10.5194/bg-2019-389
Preprint. Discussion started: 4 November 2019

not prominent (Guthruf et al., 1999). It can be expected that the lake had low nutrient loads from the catchment drainage during this period. Lake Burgäschi is classified as naturally oligotrophic based on morphometric parameters (LAWA, 1998) to naturally mesotrophic according to Binderheim-Bankay (1998). Therefore, at the times of Zone I, Lake Burgäschi was likely in low trophic levels with a possible oligotrophic-mesotrophic condition.

The transition to Zone II (~1926-1960) was marked by generally increased sedimentary green-pigments and $CaCO_3$ contents (Fig. 4 and 5), indicating enhanced lake primary productivity. The slightly decreased TOC/TN ratio also suggests a likely rise in autochthonous organic matter proportion (Meyers and Ishiwatari, 1993). The first two algal blooms (peaks of green-pigments index; Fig. 3d) imply a very likely mesotrophic to eutrophic state of the lake. Indeed, the study of Büren (1949) revealed that in 1943-1945, the trophic state of Lake Burgäschi had already shifted between mesotrophic and eutrophic.

In Zone III (~1960-1977), continuously increasing green-pigments concentrations and several algal bloom events reveal strong positive trends in lake eutrophic levels. The significant eutrophication in Lake Burgäschi might have caused intensified $CaCO_3$ precipitation and sulfur (S) deposition to sediments (Fig. 4 and 5), which is in agreement with the findings from many other eutrophic lakes (Bonk et al., 2016; Holmer and Storkholm, 2001; Schneider et al., 2018).

During Zone IV (1977-2017), we interpret that Lake Burgäschi was in highly eutrophic conditions, based on constantly high green-pigments index values and multiple prominent algal blooms (Fig. 4). Low and decreasing TOC/TN ratio values (< 10) in this zone suggest a dominant source of organic matter in sediments from aquatic primary production, which has been interpreted as a signal of eutrophic waters (Enters et al., 2006). Our interpretation is further supported by high chlorophyll-*a* concentrations in surface waters (>8 ug L^{-1}; Markus, 2007) and the dominance of blue-green algae in the phytoplankton biomass during 1977 to 1992, which characterized Lake Burgäschi as highly eutrophic (Guthruf et al., 2013; Markus, 1995).

5.2 Reconstruction of hypolimnetic oxygenation regimes of Lake Burgäschi

A large number of studies have used the proxy of Fe/Mn ratios in sediments to reconstruct past water oxygenation and mixing regimes of the lake, such as Frugone-Álvarez et al. (2017), Mackereth (1966), and Żarczyński et al. (2019) etc. However, this proxy and its interpretation are limited to cases in which the annual cycle of Fe and Mn deposition in lakes is mostly driven by redox changes in the hypolimnion and related diagenetic processes in surface sediments instead of driven by terrestrial inputs (Boyle, 2001; Naeher et al., 2013). In Lake Burgäschi, during Zone I to III, Mn and Fe were mostly independent of erosion indicators as shown in Fig. S5b. Furthermore, Van Raden (2012) has revealed that the presence of Mn-rich laminae in sediments of Lake Burgäschi can indicate frequent short-term wind-induced mixing events in the lake. Therefore, we suggest that the deposition of Fe and Mn during these three zones was mainly controlled by in-lake processes. Fe/Mn ratios together with Mn precipitation is reliably tracking past changes of hypolimnetic oxygenation of Lake Burgäschi.

In Zone I (pre ~1926), the sediments feature well-preserved Mn-Fe rich laminations and very low Fe/Mn ratios (Fig. 3 and 4), suggesting that the lake hypolimnion was seasonally well-oxygenated. The similar occurrence of

https://doi.org/10.5194/bg-2019-389
Preprint. Discussion started: 4 November 2019

visible Mn-and Fe rich laminae in sediments were also reported by Rey et al. (2017) and Van Raden (2012) in Lake Burgäschi and from other lakes, for example, Lake of the Clouds in the US (Anthony, 1977), Lake Cadagno in the Swiss Alps (Wirth et al., 2013), and Lake Żabińskie in Poland (Żarczyński et al., 2018). They revealed that the red-orange Mn-rich layers mostly consist of authigenic rhodochrosite ($MnCO_3$) that was formed when Mn-rich anoxic bottom waters are mixed with oxygenated surface waters for short intervals. The preservation of this Mn-rich layer is only possible when its sedimentation process exceeds the release process under anoxic hypolimnetic conditions (Stevens et al., 2000). Therefore, during this period, short-term mixing events and associated oxygenation may have occured during overall stratified or anoxic conditions in the hypolimnion.

In Zone II (~1926-1960), the higher Fe/Mn ratios and very low Mn- and autochthonous Fe (Fe/Ti) amounts are interpreted as the results of stable anoxic hypolimnetic waters. The formation and preservation of Fe-and Mn-oxides in sediments can be largely prevented under long-term stratification/reducing conditions (Stevens et al., 2000). The lake most likely developed anoxic hypolimnetic conditions with yearly incomplete or missing circulation in the hypolimnion.

In Zone III (1960-1977), overall decreased Fe/Mn ratios combined with reappearing Mn-and Fe-rich laminations reflects better short-term oxic conditions in hypolimnetic waters than in Zone II. However, during ~1970 to 1977, Fe/Mn ratios gradually increased (Fig. 4), which points to less oxic conditions in the hypolimnion. It seems to be related to synchronously progressive lake eutrophication. Higher primary productivity and strengthened anoxia in the hypolimnion are commonly observed in stratified lakes (Giguet-Covex et al., 2010; Mikomägi et al., 2016). Higher lake primary productivity increases high-rate aerobic degradation of organic matter and, consequently, oxygen-depletion in the hypolimnion and sediments (Gächter and Müller, 2003; Nürnberg, 2007).

Finally, in Zone IV (1977- 2017) Fe/Mn ratios proxy is no longer valid to indicate hypolimnetic oxygenation regime, as suggested by predominatly terrestrial sources of sediment Fe and Mn (Fig. S5b). Nevertheless, the well-preserved laminated sediments during this period are a clear sign of no benthic bioturbation and thus represent an indicator of generally strong anoxic conditions in hypolimnetic waters, occurring simultaneously with a highly eutrophic period. According to the limnological monitoring data of Lake Burgäschi between 1978 and 2007 (Markus, 2007), the lake water was completely anoxic at depths below 20 m during the summer-autumn stratification; even during winter circulation of most years, the lake water was still not completely mixed.

5.3 Phosphorus composition and factors controlling long-term P-fraction retention in sediments

Prior to 1977 (i.e. Zones I-III), NaBD-TP (redox-sensitive Fe- and Mn bound P) and NaOH-TP (partly non-reducible Fe oxides-P) fractions were the primary P forms in sediments of Lake Burgäschi. This seems to compare well with the study of Moosmann et al. (2006), who suggested that sediment Fe contents controls P retention in sediments of the Swiss Plateau lakes. However, after ~1977, we observed a change to predominantly Ca-P (apatite-P), occurring concurrently with considerable $CaCO_3$ precipitation during this highly eutrophic period (Fig. 4; Sect. 5.1). We interpret this as an incidence of biologically driven co-precipitation of Ca and P in highly productive

https://doi.org/10.5194/bg-2019-389
Preprint. Discussion started: 4 November 2019

lakes. The phenomenon of Ca-P co-precipitation has been observed and studied in many calcareous lakes (Dittrich and Koschel 2002; Whitehouse, 2010), and is assumed to be responsible for the scavenging of dissolved P from surface waters of eutrophic lakes (Hamilton et al., 2009). Furthermore, large amounts of Ca-P in surface sediments (top 21 cm) can act as a potential negative feedback to eutrophication in Lake Burgäschi. This is because Ca-P is relatively stable in sediments and has low potentials of P-release from surface sediments back to lake waters.

In the sediment profile of this study (coving more than 100 years), retention of total P and labile P fractions was mainly controlled by autochthonous Fe (Fe/Ti), Mn, and hypolimnetic oxygenation proxy (Fig. 7). Our results support the previous suggestion that long-term permanent sediment-P retention is largely limited by the sediment's binding capacity in anoxic conditions (Hupfer and Lewandowski, 2008; Moosmann et al., 2006), which, specifically in our case, is determined by redox-sensitive elements (autochthonous Fe and Mn) preserved in sediments. These findings are discussed in the context of each cluster zone as follows. During Zone I and Zone III, when the hypolimnion had better oxic conditions (see Sect. 5.2), the increased retention of Mn and Fe, and labile P fractions occurred simultaneously (Fig. 4 and 5). This phenomenon might be caused by efficient P-trapping in Mn- and Fe enriched layers. It has been suggested that the formation of laminated Mn- and Fe enriched layers could serve as a protective cap to reduce P release from surface sediment layers to the anoxic hypolimnion (Żarczyński et al., 2018), which thus can help improve P retention within these sedimentary layers. In Zone II, small amounts of labile P fractions might result from reduced P-bearing solid phases (Mn and Fe oxyhydroxides) in sediments under more anoxic conditions in the hypolimnion (higher Fe/Mn ratios; Sect. 5.2). In Zone IV, however, the lowest retention of total P and labile P fractions in recent sediments was noteworthy (Fig. 5 and 6). We interpret this as a combined result of eutrophication-induced hypolimnetic anoxia and lake restoration by discharge of P-rich hypolimnetic water since 1977. On the one hand, under stable anoxic conditions in the hypolimnion caused by strong eutrophication, reduced Mn and Fe preservation (Fig. 4) suggests a low capacity of permanent P-trapping within the anoxic sediments. On the other hand, hypolimnetic withdrawal restoration in Lake Burgäschi has substantially reduced hypolimnetic P concentrations by a factor of 5-6 since 1978 (Markus, 2007). This indicates a concomitant decrease in sediment-P release to the hypolimnion and P sedimentation to water-sediment interface as well. Consequently, decreased P retention in sediments was observed.

In the whole sediment profile, HCl-P and Ref.-P_o fractions had mainly autochthonous origins (Fig. 7). HCl-P fraction retention, to a large extent, resulted from authigenic $CaCO_3$-P precipitation, and increased with higher eutrophic levels in Zone III and IV (Fig. 5; Sect. 5.1). Interestingly, HCl-P fraction retention in sediments was generally lower in Zone IV (Fig. 5) than in Zone III, although the lake in Zone IV had relatively higher eutrophic levels. The pH in the hypolimnion of Lake Burgäschi varied between 7.0 and 7.5 according to the monitoring data in 1993, 2003, and 2013 (Guthruf et al., 2013). Therefore, the acid dissolution of Ca-P in hypolimnion and at the water-sediment interface is small and unlikely significant during Zone IV. The generally decreased Ca-P retention was seemingly related to the lower water-P concentrations due to hypolimnetic withdrawal as discussed above, thus resulting in smaller amounts of $CaCO_3$-P co-precipitation in the epilimnion. Overall, Ref.-P_o fraction retention in the sedimentary profile shows less variability compared with other P fractions (Fig. 5). Nevertheless, in the upper sediments (top 12 cm; Fig. 5) the enhanced retention of Ref.-P_o fraction could be derived from increased algal refractory organic matter.

https://doi.org/10.5194/bg-2019-389
Preprint. Discussion started: 4 November 2019

The interesting fact is that the water-P reductions caused by the hypolimnetic withdrawal in Lake Burgäschi have been ineffective in reducing algal blooms and curbing eutrophication. Similar findings were also reported from some lakes in Europe and the US (Kosten et al., 2012; Kolzau et al., 2014; Fastner et al., 2016). These authors have attributed this phenomenon to insufficient P-load reduction, higher water temperatures under global warming of the last few decades, and the light or nitrogen limitation of surface-water phytoplankton. We suggest that these factors mentioned may also play a role in promoting currently high primary productivity in Lake Burgäschi, but the main driver is, to our knowledge, unclear.

6 Conclusion

The primary productivity of Lake Burgäschi started to increase from the 1930s and the eutrophication proceeded since the 1960s. The hypolimnion oxygenation regime of Lake Burgäschi was characterized by four major phases since the early 1900s. Persistent anoxic conditions in the hypolimnion after ~1977 coincide with highly eutrophic conditions.

The dominant factor controlling the long-term retention of labile P-fractions and total P in sediments of Lake Burgäschi was found to be autochthonous Fe and Mn contents in anoxic sediments, which were controlled by redox conditions in the hypolimnion. Importantly, we found substantially decreased retention of labile P fractions and total P after ~1977. We attributed this phenomenon to a combined result of eutrophication-induced anoxic conditions in the hypolimnion and hypolimnetic withdrawal restoration. The former reduced the P-binding capacity (Mn and Fe oxyhydroxides) of sediments and the latter has decreased hypolimnetic P-concentrations (external P loading). By contrast, refractory Ca-P fraction predominated in surface sediments after ~1977, which indicates a decreased sediment-P availability and potential of sediment- P release (internal P loading). These results together imply that although hypolimnetic withdrawal can effectively reduce external and internal P loadings in Lake Burgäschi, it still has no significant impact on decreasing eutrophication. We attribute the delaying of lake recovery to various factors such as still high nutrient inputs from the nearby or surrounding agricultural area, light and/or nitrogen limitation to lake phytoplankton, and warmer lake temperature due to global warming. This study calls for consistently more effective measures to minimize external P loadings from the catchment, such as optimizing fertilizer application practices and technical measures in the settlement drainages.

Data availability

The data will be made available at on PANGAEA after the manuscript is published.

Author contributions

L.T. helped with sample collection, analyzed the sediment, conducted data analysis, wrote the manuscript, and acquired the funding for the project.

https://doi.org/10.5194/bg-2019-389
Preprint. Discussion started: 4 November 2019

455 P. Z. helped with sediment core subsampling, conducted the hyperspectral imaging (HSI) scanning and XRF-
456 scanning, substantially contributed to the data interpretation.
457 S.S. measured gamma-spectroscopy radiometric activities, generated the data for chronology and helped with
458 data interpretation.
459 R.L. conducted the XRF-scanning and helped with data interpretation.
460 M.G. designed the study, helped discussing the results and supervised the project.
461 All authors commented on the manuscript and approved the final version of the manuscript.
462
463 **Competing interests**
464 The authors declare that they have no conflict of interest.
465
466 **Acknowledgements**
467 We thank Stamatina Makri and Dr. Andre F. Lotter for their help during the fieldwork. We thank Irene Brunner,
468 Patrick Neuhaus, Dr. Daniela Fischer and Andrea Sanchini for their expertise and the lab assistance. Further, we
469 acknowledge Dr. Klaus A. Jarosch for the valuable suggestions about phosphorus data. The project was funded
470 by the Swiss National Science Foundation under the grant number 200021-172586, a Fellowship Grant from the
471 Chinese Scholarship Counsel and the International PhD Fellowship from University of Bern.
472

473 **References**

474 Anthony, R. S.: Iron-rich rhythmically laminated sediments in Lake of the Clouds, northeastern Minnesota, Limnol.
475 Oceanogr., 22, 45-54, https://doi.org/10.4319/lo.1977.22.1.0045, 1977.
476 Appleby, P.G.: Chronostratigraphic techniques in recent sediments, In: Tracking Environmental Change Using
477 Lake Sediments. Basin Analysis, Coring, and Chronological Techniques, edited by: Last, W.M., and Smol, J.P.,
478 Springer, Dordrecht, Netherlands, 171-203, https://doi.org/10.1007/0-306-47669-X_9, 2002.
479 Bennett, K. D.: Determination of the number of zones in a biostratigraphical sequence, New Phytol., 132, 155-
480 170, https://doi.org/10.1111/j.1469-8137.1996.tb04521.x, 1996.
481 Binderheim-Bankay, E. A.: Sanierungsziel für natürlich eutrophe Kleinseen des Schweizer Mittellandes, Ph.D.
482 thesis, ETH Zurich, Switzerland, 149 pp., 1998.
483 Bonk, A., Kinder, M., Enters, D., Grosjean, M., Meyer-Jacob, C. and Tylmann, W.: Sedimentological and
484 geochemical responses of Lake Żabińskie (north-eastern Poland) to erosion changes during the last millennium, J.
485 Paleolimnol., 56, 239-252, https://doi.org/10.1007/s10933-016-9910-6, 2016.
486 Boyle, J. F.: Inorganic Geochemical Methods in Palaeolimnology, In: Tracking Environmental Change Using Lake
487 Sediments. Basin Analysis, Coring, and Chronological Techniques, edited by: Last, W.M., and Smol, J.P., Springer,
488 Dordrecht, Netherlands, 83-141, https://doi.org/10.1007/0-306-47670-3_5, 2002.
489 Büren, G. von: Der Burgäschisee, Mitteilungen der Naturforschenden Gesellschaft, Bern, 83pp.,1949.
490 Burley, K.L., Prepas, E.E. and Chambers, P.A.: Phosphorus release from sediments in hardwater eutrophic lakes:
491 the effects of redox-sensitive and-insensitive chemical treatments, Freshwater Biol., 46, 1061-1074,
492 https://doi.org/10.1046/j.1365-2427.2001.00789.x, 2001.

https://doi.org/10.5194/bg-2019-389
Preprint. Discussion started: 4 November 2019

493 Butz, C., Grosjean, M., Fischer, D., Wunderle, S., Tylmann, W. and Rein, B.: Hyperspectral imaging spectroscopy:
494 a promising method for the biogeochemical analysis of lake sediments, J. Appl. Remote Sens. 9, 1–20,
495 https://doi.org/10.1117/1.JRS.9.096031, 2015.
496 Butz, C., Grosjean, M., Goslar, T. and Tylmann, W.: Hyperspectral imaging of sedimentary bacterial pigments: a
497 1700-year history of meromixis from varved Lake Jaczno, northeast Poland, J. Paleolimnol., 58, 57-72,
498 https://doi.org/10.1007/s10933-017-9955-1, 2017.
499 Chen, M., Ding, S., Chen, X., Sun, Q., Fan, X., Lin, J., Ren, M., Yang, L. and Zhang, C.: Mechanisms driving
500 phosphorus release during algal blooms based on hourly changes in iron and phosphorus concentrations in
501 sediments, Water res., 133, 153-164. https://doi.org/10.1016/j.watres.2018.01.040, 2018.
502 Dittrich, M. and Koschel, R.: Interactions between calcite precipitation (natural and artificial) and phosphorus
503 cycle in the hardwater lake, Hydrobiologia, 469, 49–57, https://doi.org/10.1023/A:1015571410442, 2002.
504 Einsele, W.: Über die Beziehungen des Eisenkreislaufs zum Phosphatkreislauf im eutrophen See, Arch. Hydrobiol.,
505 29, 664–686, 1936.
506 Einsele, W.: Über chemische und kolloidchemische Vorgänge in Eisen-Phosphat-Systemen unter limnischen and
507 limnogeologischen Gesichtpunkten, Arch. Hydrobiol., 33, 361–387, 1938.
508 Enters, D., Lücke, A. and Zolitschka, B.: Effects of land-use change on deposition and composition of organic
509 matter in Frickenhauser See, northern Bavaria, Germany, Sci. Total Environ., 369,178-187,
510 https://doi.org/10.1016/j.scitotenv.2006.05.020, 2006.
511 Fastner, J., Abella, S., Litt, A., Morabito, G., Vörös, L., Pálffy, K., Straile, D., Kümmerlin, R., Matthews, D.,
512 Phillips, M.G. and Chorus, I.: Combating cyanobacterial proliferation by avoiding or treating inflows with high P
513 load—experiences from eight case studies, Aquat. Ecol., 50, 367-383, https://doi.org/10.1007/s10452-015-9558-
514 8, 2016.
515 Frugone-Álvarez, M., Latorre, C., Giralt, S., Polanco-Martínez, J., Bernárdez, P., Oliva-Urcia, B., Maldonado, A.,
516 Carrevedo, M.L., Moreno, A., Delgado Huertas, A. and Prego, R.: A 7000-year high-resolution lake sediment
517 record from coastal central Chile (Lago Vichuquén, 34° S): implications for past sea level and environmental
518 variability, J. Quaternary Sci., 32, 830-844, https://doi.org/10.1002/jqs.2936, 2017.
519 Gächter, R.: Lake restoration. Why oxygenation and artificial mixing cannot substitute for a decrease in the
520 external phosphorus loading, Aquat. Sci., 49, 176–185, https://doi.org/10.1007/BF02538501, 1987.
521 Gächter, R. and Wehrli, B.: Ten years of artificial mixing and oxygenation: no effect on the internal phosphorus
522 loading of two eutrophic lakes, Environ. Sci. Technol., 32, 3659–3665, https://doi.org/10.1021/es980418, 1998.
523 Gächter, R. and Müller, B.: Why the phosphorus retention of lakes does not necessarily depend on the oxygen
524 supply to their sediment surface, Limnol. Oceanogr., 48, 929-933, https://doi.org/10.4319/lo.2003.48.2.0929, 2003.
525 Giguet-Covex, C., Arnaud, F., Poulenard, J., Enters, D., Reyss, J.L., Millet, L., Lazzaroto, J. and Vidal, O.:
526 Sedimentological and geochemical records of past trophic state and hypolimnetic anoxia in large, hard-water Lake
527 Bourget, French Alps, J. Paleolimnol., 43, 171-190, https://doi.org/10.1007/s10933-009-9324-9, 2010.
528 Gonsiorczyk, T., Casper, P., and Koschel, R.: Phosphorus-binding forms in the sediment of an oligotrophic and an
529 eutrophic hardwater lake of the Baltic Lake District (Germany), Water Sci. Technol., 37, 51–58,
530 https://doi.org/10.1016/S0273-1223(98)00055-9, 1998.
531 Grimm, E. C.: CONISS: a FORTRAN 77 program for stratigraphically constrained cluster analysis by the method
532 of incremental sum of squares, Comput. Geosci., 13,13–35, https://doi.org/10.1016/0098-3004(87)90022-7, 1987.

https://doi.org/10.5194/bg-2019-389
Preprint. Discussion started: 4 November 2019

Guthruf, J., Zeh, M. and Guthruf-Seiler, K.: Kleinseen im Kanton Bern, Water Protection and Waste Management Office of the Canton of Bern, Bern, 1999.

Guthruf, K., Maurer, V., Ryser, R., Zeh, M., and Zweifel, N.: Zustand der Kleinseen, Construction, Transport and Energy Directorate of the Canton of Bern Office for Water and Waste Water and soil protection laboratory, Bern, 2013.

Håkanson, L., and Jansson, M. (Eds.) : Principles of Lake Sedimentology, The Blackburn Press, New Jersey, USA, 2002.

Hamilton, S.K., Bruesewitz, D.A., Horst, G.P., Weed, D.B. and Sarnelle, O.: Biogenic calcite–phosphorus precipitation as a negative feedback to lake eutrophication, Can. J. Fish. Aquat. Sci., 66, 343-350, https://doi.org/10.1139/F09-003, 2009.

Heiri, O., A. F. Lotter, and Lemcke, G.: Loss on ignition as a method for estimating organic and carbonate content in sediments: reproducibility and comparability of results, J. Paleolimnol., 25, 101-110, https://doi.org/10.1023/A:1008119611481, 2001.

Holmer, M., and Storkholm, P.: Sulphate reduction and sulphur cycling in lake sediments: a review, Freshwater Biol., 46, 431-451, https://doi.org/10.1046/j.1365-2427.2001.00687.x, 2001.

Hupfer, M. and Lewandowski, J.: Oxygen controls the phosphorus release from lake sediments–a long-lasting paradigm in limnology, Int. Rev. Hydrobiol., 93, 415-432, https://doi.org/10.1002/iroh.200711054, 2008.

Juggins, S.: rioja: analysis of quaternary science data, https://cran.r-project.org/web/packages/rioja/index.html, 2017.

Kolzau, S., Wiedner, C., Rücker, J., Köhler, J., Köhler, A. and Dolman, A. M.: Seasonal patterns of nitrogen and phosphorus limitation in four German lakes and the predictability of limitation status from ambient nutrient concentrations, Plos One, 9, e96065, https://doi.org/10.1371/journal.pone.0096065, 2014.

Kosten, S., Huszar, V.L., Bécares, E., Costa, L.S., van Donk, E., Hansson, L.A., Jeppesen, E., Kruk, C., Lacerot, G., Mazzeo, N. and De Meester, L.: Warmer climates boost cyanobacterial dominance in shallow lakes, Global, Change Biol., 18, 118-126, https://doi.org/10.1111/j.1365-2486.2011.02488.x, 2012.

Kucklentz, V. and Hamm, A. (Eds.): Möglichkeiten und Erfolgsaussichten der Seenrestaurierung, Bayrische Landesanstalt für Wasserforschung, München, Germany, 212 pp., 1988.

LAWA (Länderarbeitsgemeinschaft Wasser): Gewässerbewertung — stehende Gewässer: Richtlinie für die Bewertung nach trophischen Kriterien, Germany, 1998.

Lukkari, K., Hartikainen, H. and Leivuori, M.: Fractionation of sediment phosphorus revisited. I: Fractionation steps and their biogeochemical basis, Limnol. Oceanog-Meth., 5,433-444, https://doi.org/10.4319/lom.2007.5.433, 2007.

Mackereth, F.J.H.: Some chemical observations on post-glacial lake sediments, Philos. T. Roy. Soc. B., 250,165-213, https://doi.org/10.1098/rstb.1966.0001, 1966.

Markus, Z.: Resultate der Wasser- und Planktonuntersuchungen 1977-1995, Office for Water Protection and Waste Management of the Canton of Bern, Bern, 1995.

Markus, Z.: 30 Jahre Tiefenwasser-Ableitung Wie geht es dem Burgäschisee heute?, Office for Water Protection and Waste Management of the Canton of Bern, Bern, 2007.

McCulloch, J., A. Gudimov, G. Arhonditsis, A. Chesnyuk, and Dittrich, M.: Dynamics of P-binding forms in sediments of a mesotrophic hard-water lake: Insights from non-steady state reactive-transport modeling, sensitivity and identifiability analysis, Chem. Geol., 354,216-232, https://doi.org/10.1016/j.chemgeo.2013.06.011, 2013.

Meyers, P. A., and Ishiwatari, R.: Lacustrine organic geochemistry—an overview of indicators of organic matter sources and diagenesis in lake sediments, Org. Geochem., 20, 867-900, http://dx.doi.org/10.1016/0146-6380(93)90100-P, 1993,

Michel, H., Barci-Funel, G., Dalmasso, J., Ardisson, G., Appleby, P., Haworth, E. and El-Daoushy, F.: Plutonium, americium and cesium records in sediment cores from Blelham Tarn, Cumbria (UK), J. Radioanal. Nucl. Ch., 247, 107-110, https://doi.org/10.1023/A:1006719215833, 2001.

Moosmann, L., R. Gächter, B. Müller, and Wüest, A.: Is phosphorus retention in autochthonous lake sediments controlled by oxygen or phosphorus?, Limnol. Oceanogr., 51, 763-771, https://doi.org/10.4319/lo.2006.51.1_part_2.0763, 2006.

Mikomägi, A., Koff, T., Martma, T. and Marzecová, A.: Biological and geochemical records of human-induced eutrophication in a small hard-water lake, Boreal Env. Res., 21, 513-527, 2016.

Naeher, S., Gilli, A., North, R.P., Hamann, Y. and Schubert, C.J.: Tracing bottom water oxygenation with sedimentary Mn/Fe ratios in Lake Zurich, Switzerland, Chem. Geol., 352, 125-133, https://doi.org/10.1016/j.chemgeo.2013.06.006, 2013.

Nikolai, S.J. and Dzialowski, A.R.: Effects of internal phosphorus loading on nutrient limitation in a eutrophic reservoir, Limnologica, 49, 33-41, https://doi.org/10.1016/j.limno.2014.08.005, 2014.

Nürnberg, G.K.: Lake responses to long-term hypolimnetic withdrawal treatments, Lake Reserv. Manage., 23,388-409, https://doi.org/10.1080/07438140709354026, 2007.

Ogdahl, M. E., Steinman, A. D. and Weinert, M. E.: Laboratory-determined phosphorus flux from lake sediments as a measure of internal phosphorus loading, Jove-J. Vis. Exp., 85, 51617, https://dx.doi.org/10.3791%2F51617, 2014.

Oksanen, J., Blanchet, F.G., Kindt, R., Legendre, P., Minchin, P.R., O'hara, R., Simpson, G.L., Solymos, P., Stevens, M.H.H. and Wagner, H.: Package 'vegan'. Community ecology package, version 2, http://cran.r-project.org/web/packages/vegan/index.html, 2013.

Pennington, W., Tutin, T.G., Cambray, R.S. and Fisher, E.M.: Observations on lake sediments using fallout ^{137}Cs as a tracer, Nature, 242, 324–326, https://doi.org/10.1038/242324a0, 1973.

R Development Core Team: R: A Language and Environment for Statistical Computing, R Foundation for Statistical Computing, Vienna, Austria, 2017.

Rentz, J., Turner, I.P. and Ullman, J.L.: Removal of phosphorus from solution using biogenic iron oxides, Water Res. 43, 2029-2035, https://doi.org/10.1016/j.watres.2009.02.021, 2009.

Rey, F., Gobet, E., van Leeuwen, J.F.N., Gilli, A., van Raden, U.J., Hafner, A., Wey, O., Rhiner, J., Schmocker, D., Zünd, J., Tinner, W.: Vegetational and agricultural dynamics at Burgäschisee (Swiss Plateau) recorded for 18,700 years by multi-proxy evidence from partly varved sediments, Veg. Hist. Archaeobot., 26, 571–586. https://doi.org/10.1007/s00334-017-0635-x, 2017.

Ribeiro, D., Martins, G., Nogueira, R., Cruz, J.V., and Brito, A.: Phosphorus fractionation in volcanic lake sediments (Azores–Portugal), Chemosphere, 70, 1256–1263, https://doi.org/10.1016/j.chemosphere.2007.07.064, 2008.

https://doi.org/10.5194/bg-2019-389
Preprint. Discussion started: 4 November 2019

Richter, T.O., Van der Gaast, S., Koster, B., Vaars, A., Gieles, R., de Stigter, H.C., De Haas, H. and van Weering, T.C.: The Avaatech XRF Core Scanner: technical description and applications to NE Atlantic sediments, Geol. Soc. London Spec. Publ., 267, 39-50, https://doi.org/10.1144/GSL.SP.2006.267.01.03, 2006.

Rydin, E.: Potentially mobile phosphorus in Lake Erken sediment. Water Res., 34, 2037–2042, https://doi.org/10.1016/S0043-1354(99)00375-9, 2000.

Schmid, S.M., Fügenschuh, B., Kissling, E. and Schuster, R.: Tectonic map and overall architecture of the Alpine orogen, Eclogae Geol. Helv., 97, 93-117, https://doi.org/10.1007/s00015-004-1113-x, 2004.

Schneider, T., Rimer, D., Butz, C.,and Grosjean, M.: A high-resolution pigment and productivity record from the varved Ponte Tresa basin (Lake Lugano, Switzerland) since 1919: insight from an approach that combines hyperspectral imaging and highperformance liquid chromatography, J. Paleolimnol., 60, 381–398, https://doi.org/10.1007/s10933-018-0028-x. 2018.

Schnurrenberger, D., Russell, J. and Kelts, K.: Classification of lacustrine sediments based on sedimentary components, J. Paleolimnol., 29,141–154, https://doi.org/10.1023/A:1023270324800, 2003.

Smith, L., . Watzin, M. C. and and Druschel, G.: Relating sediment phosphorus mobility to seasonal and diel redox fluctuations at the sediment-water interface in a eutrophic freshwater lake, Limnol. and Oceanogr., 56, 2251-2264, https://doi.org/10.4319/lo.2011.56.6.2251, 2011.

Stevens, L., Ito, E. and Olson, D.: Relationship of Mn-carbonates in varved lake-sediments to catchment vegetation in Big Watab Lake, MN, USA. J. Paleolimnol., 24,199–211, https://doi.org/10.1023/A:1008169526577, 2000.

Trolle, D., Hamilton, D.P., and Pilditch, C.A.: Evaluating the influence of lakemorphology, trophic status and diagenesis on geochemical profiles in lake sediments, Appl. Geochem., 25, 621–632, https://doi.org/10.1016/j.apgeochem.2010.01.003, 2010.

Tu, L., Jarosch, K.A., Schneider, T. and Grosjean, M.: Phosphorus fractions in sediments and their relevance for historical lake eutrophication in the Ponte Tresa basin (Lake Lugano, Switzerland) since 1959, Sci. Total Environ., 685, 806-817, https://doi.org/10.1016/j.scitotenv.2019.06.243, 2019.

Tylmann, W., Bonk, A., Goslar, T., Wulf, S. and Grosjean, M.: Calibrating ^{210}Pb dating results with varve chronology and independent chronostratigraphic markers: Problems and implications, Quat. Geochronol. 32, 1-10, https://doi.org/10.1016/j.quageo.2015.11.004, 2016.

van Raden, U. J.: High-resolution Swiss lake records of climate change. Ph.D. thesis, ETH Zurich, Switzerland, https://doi.org/10.3929/ethz-a-009783578, 2012.

Whitehouse, R.D.: Phosphorus scavenging through calcite co-precipitation: bringing clarity to Clear Lake, B.Sc. thesis, University of British Columbia, Canada, 2010.

Wirth, S.B., Gilli, A., Niemann, H., Dahl, T.W., Ravasi, D., Sax, N., Hamann, Y., Peduzzi, R., Peduzzi, S., Tonolla, M. and Lehmann, M.F.: Combining sedimentological, trace metal (Mn, Mo) and molecular evidence for reconstructing past water-column redox conditions: The example of meromictic Lake Cadagno (Swiss Alps), Geochim. Cosmochim. Ac., 120, 220-238, https://doi.org/10.1016/j.gca.2013.06.017, 2013.

Żarczyński, M., Wacnik, A. and Tylmann, W.: Tracing lake mixing and oxygenation regime using the Fe/Mn ratio in varved sediments: 2000year-long record of human-induced changes from Lake Zabinskie (NE Poland), Sci. Total Environ., 657, 585-596, https://doi.org/10.1016/j.scitotenv.2018.12.078, 2019.

https://doi.org/10.5194/bg-2019-389
Preprint. Discussion started: 4 November 2019

650 Żarczyński, M., Tylmann, W., and Goslar, T.: Multiple varve chronologies for the last 2000 years from the
651 sediments of Lake Żabińskie (northeastern Poland)–Comparison of strategies for varve counting and uncertainty
652 estimations, Quaternary Geochronology, 47, 107-119, https://doi.org/10.1016/j.quageo.2018.06.001, 2018.
653
654
655
656
657
658
659
660
661
662
663
664
665
666
667
668
669

https://doi.org/10.5194/bg-2019-389
Preprint. Discussion started: 4 November 2019

Biogeosciences
Discussions
Open Access
EGU

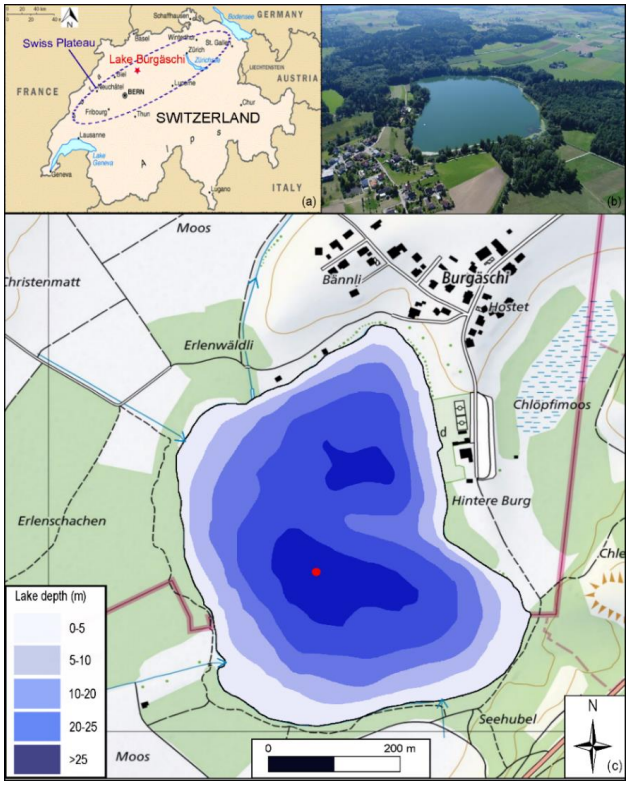

Figure 1: Study site. (a) Overview map of Switzerland and the Swiss Plateau. Lake Burgäschi is indicated as the red asterisk. (b) Satellite photo of Lake Burgäschi and catchment (© 2018 Google Maps). (c) Bathymetric map of Lake Burgäschi adapted from Guthruf et al. (1999). The red dot indicates the coring site (color figure online). Green areas around the lake indicate forests, white areas agricultural lands. Inflow and outflow to the lake are indicated by blue arrow lines (topographic maps: © swisstopo).

https://doi.org/10.5194/bg-2019-389
Preprint. Discussion started: 4 November 2019

688

689

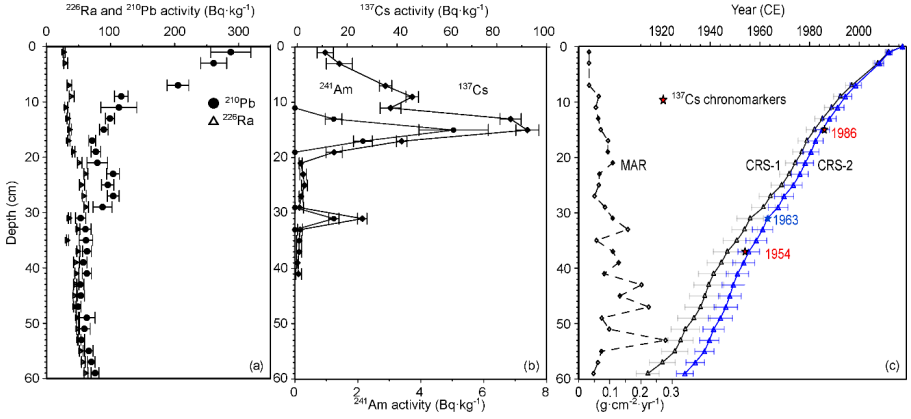

690

691 **Figure 2: (a) Total ^{210}Pb, ^{226}Ra, and (b) ^{137}Cs and ^{241}Am activity concentration profiles in sediment core Burg17-B from**
692 **Lake Burgäschi; (c) The comparison of different ^{210}Pb CRS models: unconstrained CRS -1 model and constrained CRS-**
693 **2 model at 1963; the mass accumulation rates (MAR) are obtained from the CRS -2 model.**

694

695

696

697

https://doi.org/10.5194/bg-2019-389
Preprint. Discussion started: 4 November 2019

Biogeosciences
Discussions
Open Access
EGU

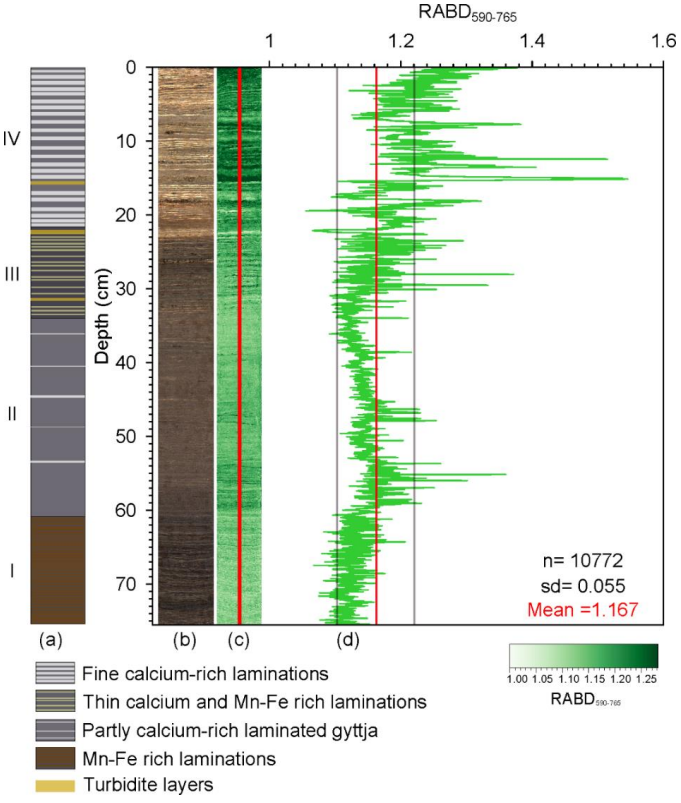

Figure 3: (a) Lithological description of Burg17-B sediment core. The intensities of Ca, Fe and Mn in each unit were inferred from XRF-element counts; Yellow colors highlight the turbidite layers identified from the XRF peaks of siliciclastic elements e.g. K, Ti, and Rb. (b) RGB contrast enhanced sediment core picture. (c) The map of the spectral index $RABD_{590-765}$ (i.e. green-pigments) distribution, and (d) the graphic output of $RABD_{590-765}$ spectral index within the boundary of the red lines (c) which shows the 2-mm wide sampling range. The red line in (d) indicates the mean index value and the grey lines represent the one-standard deviations (sd). The colorbar represents the index values of the distribution map (color figure online). n is the number of rows of the $RABD_{590-765}$ index map.

https://doi.org/10.5194/bg-2019-389
Preprint. Discussion started: 4 November 2019

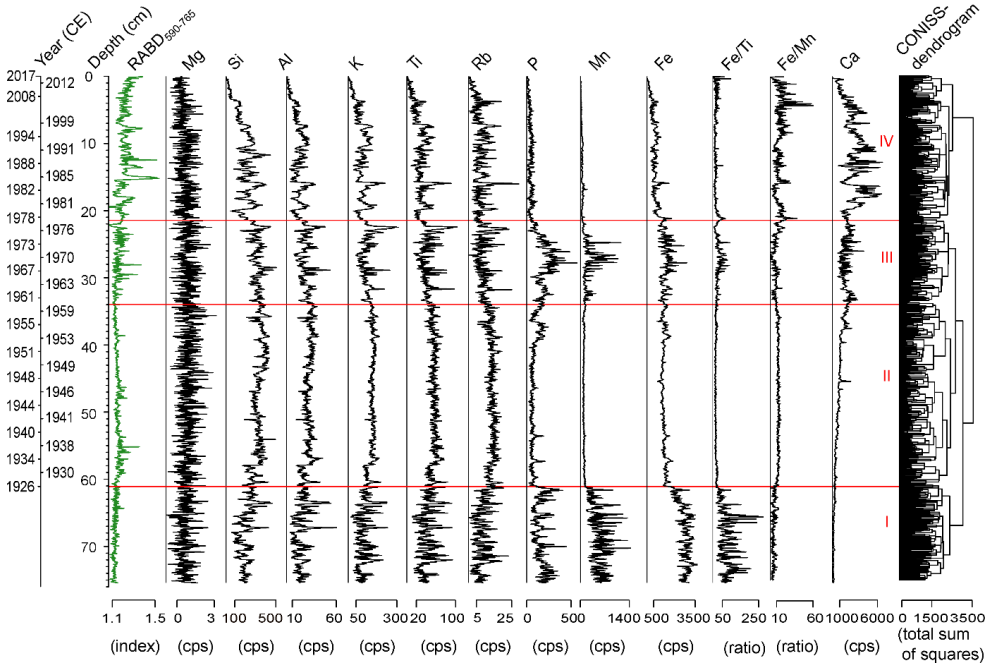

Figure 4: Stratigraphical records of HSI-inferred green-pigments ($RABD_{590-765}$) and XRF-data in sediments of Core Burg17-B. Elemental counts are represented in cps (counts per second). The red horizontal lines separate the four significant clusters retrieved by the CONISS analysis (color figure online).

https://doi.org/10.5194/bg-2019-389
Preprint. Discussion started: 4 November 2019

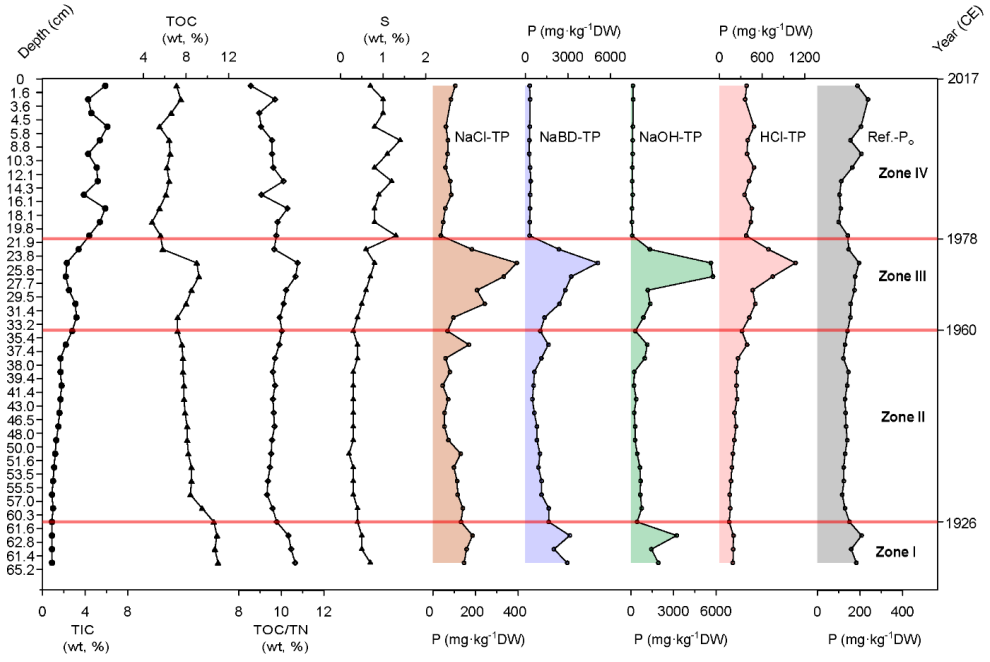

Figure 5: The stratigraphy of total inorganic carbon (TIC), total organic carbon (TOC), sulfur (S) contents, TOC/TN ratio and five phosphorus fractions in sediments of Lake Burgäschi. The y-axis (left) refers to the sediment depth of Core Burg17-B. The horizontal red lines separate the significant CONISS zones as in Fig. 4. The secondary y-axis (right) indicates approximate ages of sediment inferred from the Burg17-B core chronology.

https://doi.org/10.5194/bg-2019-389
Preprint. Discussion started: 4 November 2019

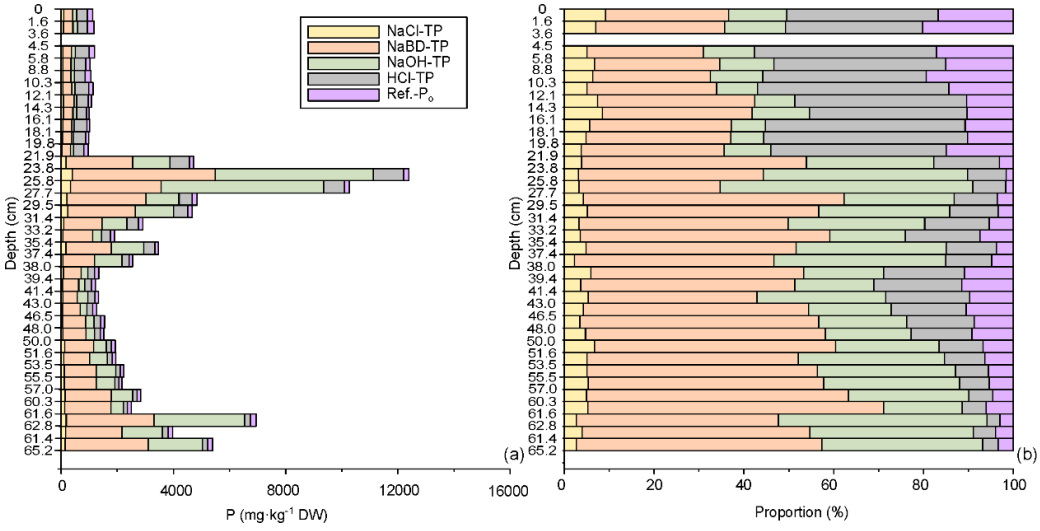

Figure 6: Vertical profile of (a) P fractions concentrations and (b) their proportions of total P in sediments. The y-axis (left) refers to the sediment depth of Core Burg17-B. Note that the sample between 3.6-4.5 cm depth was removed from dataset because the values were extremely higher than any sample data (data not shown), which is abnormal according to XRF-P counts at the corresponding depth (Fig. S3b). We attributed this to the result of contamination during the sample measurements.

https://doi.org/10.5194/bg-2019-389
Preprint. Discussion started: 4 November 2019

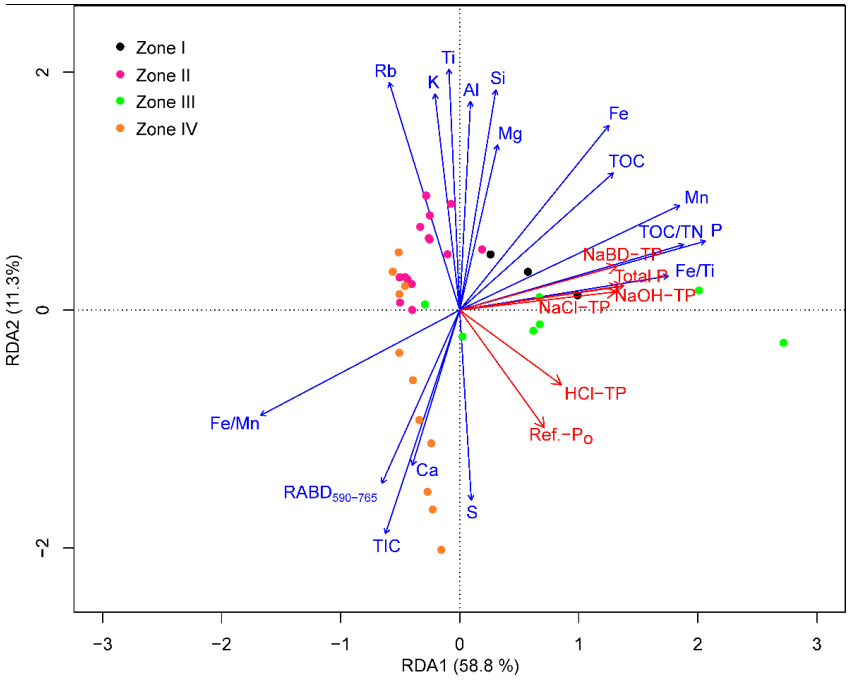

Figure 7. RDA biplot displaying correlation between response variables (P fraction dataset; red arrows) and explanatory variables (green-pigments and other geochemical records; blue arrows). The colored points represent data points of individual cluster zones.